



ELSEVIER

Physica C 270 (1996) 91–96

PHYSICA C

Critical current, film thickness and grain alignment for spray-pyrolyzed films of $TlBa_2Ca_2Cu_3O_x$

E.D. Specht ^{*,a}, A. Goyal ^a, D.M. Kroeger ^a, A. Mogro-Campero ^b,
P.J. Bednarczyk ^b, J.E. Tkaczyk ^b, J.A. DeLuca ^b

^a Oak Ridge National Laboratory, Oak Ridge, TN 37831-6118, USA

^b GE Research and Development Center, Schenectady, NY 12301, USA

Received 17 June 1996; revised manuscript received 12 August 1996

Abstract

X-ray diffraction rocking curves are used to measure the c axis alignment of $TlBa_2Ca_2Cu_3O_x$ films grown on polycrystalline substrates with thickness varying from 3 to 10.5 μm . Films thicker than 3 μm are found to contain two layers: a well aligned (3.5° FWHM) bottom layer, and a poorly aligned (greater than 12° FWHM) top layer. Azimuthal scans show that the component with good long-range out-of-plane alignment retains its characteristic colony microstructure of local in-plane alignment as film thickness increases. The length dependence of the critical current density may be accounted for by assuming that all the supercurrent is carried by the well-aligned component.

1. Introduction

While high-temperature superconductors have been produced with high current density J_c , less progress has been made in obtaining high total currents. For coevaporated $YBa_2Cu_3O_7$ (Y-123) films grown epitaxially on $SrTiO_3$ [1–3], silver-sheathed powder-in-tube $Bi_2Sr_2Ca_2Cu_3O_x$ (Bi-2223) tapes [4,5], and spray-pyrolyzed $TlBa_2Ca_2Cu_3O_x$ (Tl-1223) deposits on polycrystalline yttria-stabilized zirconia (YSZ) [6], the behavior is qualitatively similar. High J_c is observed up to some critical sample thickness t_c . Total critical current does not increase significantly as the samples are made thicker than t_c .

This limits the current per unit width, K_c ; $K_c = J_c t_c$. As shown in Table 1, K_c does not exceed 5 A/mm for any of these materials. An exception is Y-123 grown epitaxially on $SrTiO_3$ by pulsed laser deposition (PLD), which carries high J_c even in the thickest films observed [7].

Coevaporated Y-123 was found to grow up to thickness t_c with the c axis aligned with the substrate normal. Subsequent growth occurs with the a axis parallel to the substrate normal, leading to large-angle grain boundaries and reduced J_c [1–3]. Similarly, a layer of Bi-2223 with thickness $\sim t_c$ adjacent to the silver sheath was found to have better c axis alignment, accounting for its higher J_c tapes [4,5]. Again, PLD Y-123 is exceptional, retaining good c orientation for all thicknesses [7].

Tl-1223 has been shown to exhibit a dependence of J_c on film thickness qualitatively similar to co-

* Corresponding author. Fax: +1 423 574 7659;
e-mail: esy@oml.gov.

evaporated Y-123 and Bi-2223, but elucidation of the mechanism for the decrease in J_c with film thickness was deferred pending detailed microstructural investigation [6]. Here we report x-ray rocking curves on Tl-1223 films of varying thickness which show that Tl-1223 spray pyrolyzed deposits follow the behavior of Bi-2223 powder-in-tube filaments: in a layer adjacent to the substrate of thickness $t_c \sim 1.5 \mu\text{m}$, the c axes of the grains are well aligned with the substrate normal. In the rest of the film, c axis alignment is poorer.

2. Experimental

Deposition conditions were used which have been optimized to produce dense, c -oriented high J_c films which are $2.5 \mu\text{m}$ thick [6,8–13]. Ref. [6] describes film preparation for this study, and Ref. [8] gives a more general description of the spray pyrolysis deposition process for Tl-1223. Briefly, a nitrate solution of Ag-Ca-Ba-Cu-O is sprayed onto polycrystalline YSZ substrates, heat-treated in air to convert nitrates to oxides, and then heat-treated in Tl_2O vapor to form the superconductor. J_c measurements for these films are reported in Ref. [6].

X-ray measurements used a rotating anode Cu source operating at 50 kV and 200 mA. A sagittally focusing graphite monochromator selected K_α radiation. Slits defined a $2 \times 2 \text{ mm}^2$ incident beam. Rocking curves (ω scans) were measured for the Tl-1223 (0010) peak. Raw data is multiplied by $\sin \theta \cos \omega / \sin(\theta - \omega)$ to correct for scattering volume changes, where the incident and scattering beams make angles $\theta + \omega$ and $\theta - \omega$ respectively to the sample surface.

Local in-plane orientation was measured using a $0.5 \times 0.5 \text{ mm}^2$ incident beam. The sample was tilted

so that X rays reflect in the bisecting geometry (i.e. with incident and scattered beams at equal angles to the surface) from (1014) planes when the sample normal is [001]. In this geometry, a 0.37 mm^2 area is illuminated. The penetration depth is $12 \mu\text{m}$. The sample was rotated about the surface normal, giving a peak at each of the four {1014} positions. This measurements samples only those grains with their c axes within 1° of the sample normal, i.e. the component of the sample with the best out-of-plane alignment. The sample is translated between measurements to sample the entire $2 \times 4 \text{ mm}^2$ conducting path. Such measurements have been described in more detail in Refs. [10,12,14].

3. Results and discussion

Scanning electron micrographs (Fig. 1) show that the films retain their plate-like morphology at all thicknesses studied. Some coarsening of the grains with growth is evident, and close examination reveals misoriented grains which appear edge-on.

Rocking curves are shown in Fig. 2. While the $3.0 \mu\text{m}$ film's rocking curve is well-described by either a the sum of two Gaussian lineshapes (as shown) or by single lineshape with strong tails, the thicker films are clearly composed of a well-aligned and a poorly-aligned portion. Least-squares fits are shown in Fig. 2 of the rocking curve count rate i to the sum of two Gaussians,

$$i = A_1 \exp(-\omega^2/2\sigma_1^2) + A_2 \exp(-\omega^2/2\sigma_2^2). \quad (1)$$

While this decomposition is not unique, it serves to compare the rocking curves. The width of the sharp component is held fixed at $\sigma_1 = 1.5^\circ$ (FWHM =

Table 1
Critical current density, critical thickness, and critical current per unit width

Material	J_c (A/cm ²) at 77 K	t_c (μm)	K_c (A/mm)
Coevaporated Y-123 [1–3]	10^6	0.4	4
PLD Y-123 [7]	10^6	$> 2.4 \mu\text{m}$	> 24
Powder-in-tube Bi-2223 [4,5]	5×10^4	10	5
Spray-pyrolyzed Tl-1223 [6]	6×10^4	5	3

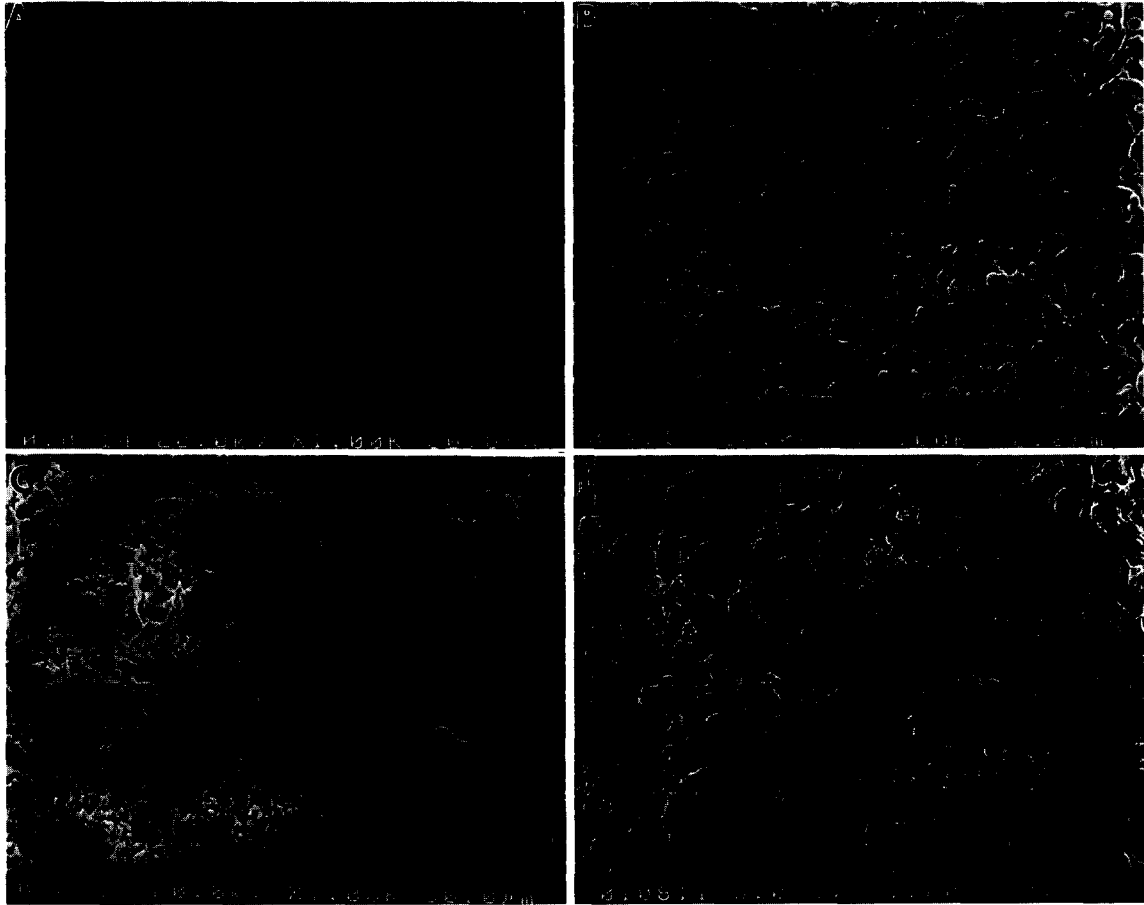


Fig. 1. Scanning electron micrographs of Tl-1223 films (A) 3.0 μm , (B) 5.2 μm , (C) 7.8 μm , and (D) 10.2 μm thick.

3.5°). The amplitudes A_1 and A_2 of the sharp and broad component and the width σ_2 of the broad component are free parameters. Because the (001) planes are tilted in two orthogonal directions (only one of which has been measured), the integrated intensity of the sharp component of the Bragg peak is equal to

$$I_1 = A_1 \int \int \exp\left[-(\omega_1^2 + \omega_2^2)^2 / 2\sigma_1^2\right] d\omega_1 d\omega_2$$

$$= 2\pi A_1 \sigma_1^2. \quad (2)$$

Similarly, the integrated intensity of the broad component is $I_2 = 2\pi A_2 \sigma_2^2$. The integrated intensity is shown in Fig. 3 for each component. Also shown is the FWHM of the broad component, equal to $2.35 \sigma_2$.

Noting the change in scale with film thickness, it is apparent in Fig. 2 that the intensity of the sharp component falls rapidly as the film becomes thicker. This decrease may be accounted for by assuming that the well-aligned layer remains unchanged as more material is deposited on top, attenuating the x-ray beam. Shown in Fig. 3a is the model curve

$$I_1 \sim \exp(-\mu t / 2 \sin \theta), \quad (3)$$

where $\mu = 1133/\text{cm}$ is the coefficient of X-ray absorption and t is the film thickness. Measurement of the integrated intensity of the broader component is subject to large uncertainty.

Unlike the sharp component, which remains unchanged as additional material is deposited, the broad component becomes increasingly misaligned, as

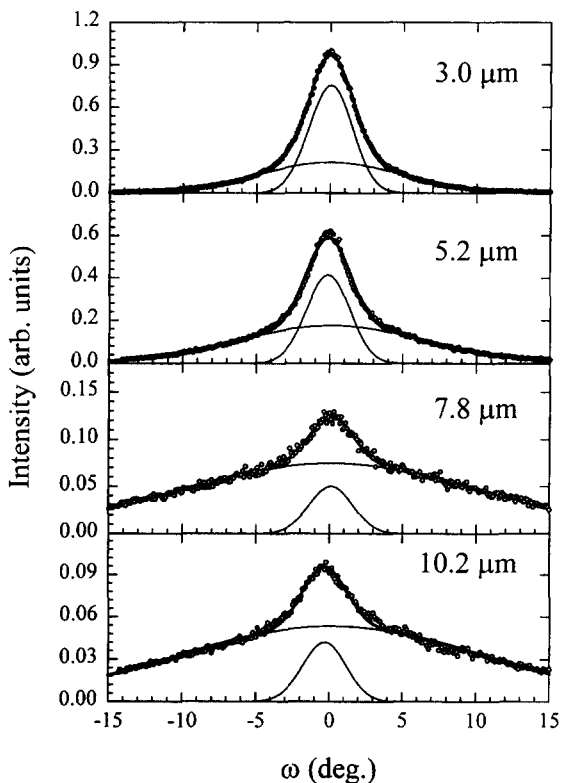


Fig. 2. X-ray rocking curves for the (0010) peak of Tl-1223 films. Solid lines are least squares fits to a sum of two Gaussians Eq. (1), one with FWHM = 3.5°, the other of variable width. Note change of scale with film thickness.

shown in Fig. 3c. We can tell whether this poorly aligned material is carrying a supercurrent by analyzing the variation in K_c with film thickness. As shown for Y-123 films [1,3], K_c will be proportional to t for films thinner than t_c and constant for films thicker than t_c . As shown in Fig. 4, this model is consistent with measured K_c for any $t_c < 3 \mu\text{m}$.

The thickness t_c of the well-aligned layer depends on the interpretation of the rocking curves. The fit shown in Fig. 1 uses a Gaussian lineshape, giving the sharp component $\sim 1/3$ of the total intensity of the $3 \mu\text{m}$ film, which implies that $t_c \sim 1 \mu\text{m}$. The rocking curves may be fit equally well, however, using a lineshape with stronger tails such as $i \sim 1/(1 + \omega^2/\kappa^2)$ (i.e. Lorentzian), in which case the $3 \mu\text{m}$ rocking curve consists of a sharp component only, and $t_c \sim 3 \mu$. We cannot use thinner films to obtain a definitive answer because thinner films do

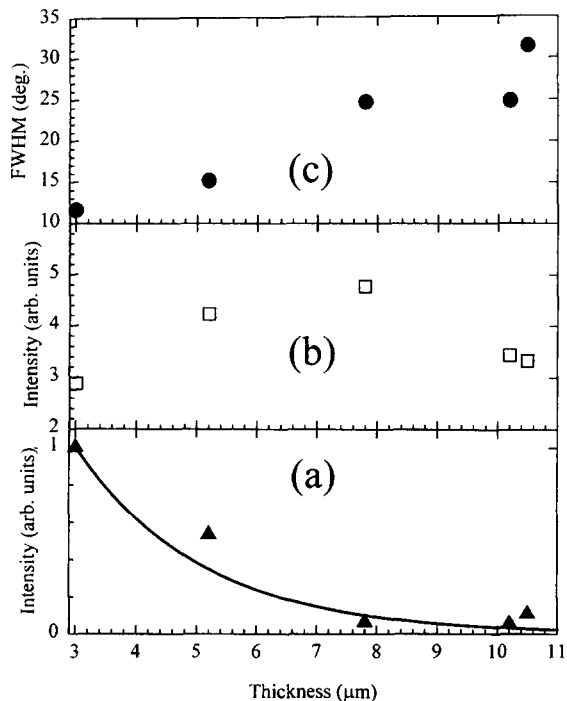


Fig. 3. Integrated intensity of (a) the sharp component and (b) the broad component and (c) FWHM of the broad component of Tl-1223 rocking curves. Solid line is a fit to Eq. (3).

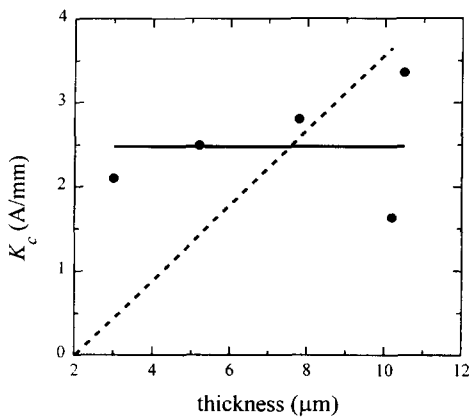


Fig. 4. Average critical current per unit width for four 1 mm long by 2 mm wide segments. Solid line: dependence for a constant-thickness film. Dashed line: dependence for a constant- J_c film.

not form a continuous superconducting layer. Microscopic examination of 3 μm films shows no evidence of poorly-aligned material at the surface [8], suggesting that t_c is closer to 3 μm than 1 μm . For this reason, it is likely that the 3 μm films are best described as a homogeneous layer (Lorentzian lineshape), while the thicker films are better described as containing two layers (two-component Gaussian lineshape).

Scans of in-plane orientation show that grains in each 0.37 mm^2 area are aligned with an average FWHM of 17° (3.0 μm) and 14° (10.5 μm) for the orientational distribution of the thinnest and thickest films — unchanged within statistical uncertainty. Shown in Fig. 5 are maps of the in-plane orientation for these films. Because these scans select those grains for which the [001] axis is aligned normal to the film, they show the orientation of the well-aligned component, which we have shown to be the layer close to the substrate. Both films exhibit the colony microstructure characteristic of thin high J_c Tl-1223 films in which colonies of grains exhibit in-plane alignment extending over ~ 1 mm [10,12,14]. It may be seen in Fig. 5 that the underlying layer of the

thicker film has better in-plane alignment than the thinner film, but this falls within the film-to-film variation seen in similarly prepared films, so the difference is not significant.

In conclusion, we have shown that J_c is reduced for thick Tl-1223 films because only a thin, well-aligned layer adjacent to the substrate carries high currents, just as for other superconducting films. The thickness dependence of K_c demonstrates that the maximum thickness t_c of the well-aligned layer is less than 3 μm . Analysis of the rocking curve of the thinnest layer shows that $t_c > 1$ μm .

Acknowledgements

Research sponsored by the U.S. Department of Energy, Office of Energy Efficiency and Renewable Energy, Office of Utility Technology-Superconductivity Program and Division of Materials Sciences. Prepared by Oak Ridge National Laboratory, managed by Lockheed Martin Energy Research Corp. for the U.S. Department of Energy under contract number DE-AC05-96OR22464.

References

- [1] F.E. Luborsky, R.F. Kwasnick, K. Borst, M.F. Garbaskas, E.L. Hall and M.J. Curran, *J. Appl. Phys.* 64 (1988) 6388.
- [2] A. Mogro-Campero, L.G. Turner, E.L. Hall, N. Lewis, L.A. Peluso and W.E. Balz, *Supercond. Sci. Tech.* 3 (1990) 62.
- [3] A. Mogro-Campero and L.G. Turner, *J. Superconduct.* 6 (1993) 37.
- [4] D.C. Larbalestier, X.Y. Cai, Y. Feng, H. Edelman, A. Umezawa, G.N.J. Riley and W.L. Carter, *Physica C* 221 (1994) 299.
- [5] G. Grasso, B. Hensel, A. Jeremie and R. Flükiger, *Physica C* 241 (1995) 45.
- [6] A. Mogro-Campero, P.J. Bednarczyk, J.E. Tkaczyk and J.A. DeLuca, *Physica C* 247 (1995) 239.
- [7] D.H. Lowndes, private communication.
- [8] J.A. DeLuca, P.L. Karas, J.E. Tkaczyk, P.J. Bednarczyk, M.F. Garbaskas, C.L. Briant and D.B. Sorensen, *Physica C* 205 (1993) 21.
- [9] A. Goyal, E.D. Specht, D.M. Kroeger, J.E. Tkaczyk, C.L. Briant and J.A. DeLuca, *Appl. Phys. Lett.* 67 (1995) 2563.
- [10] D.M. Kroeger, A. Goyal, E.D. Specht, Z.L. Wang, J.E. Tkaczyk, J.A. Sutliff and J.A. DeLuca, *Appl. Phys. Lett.* 64 (1994) 106.

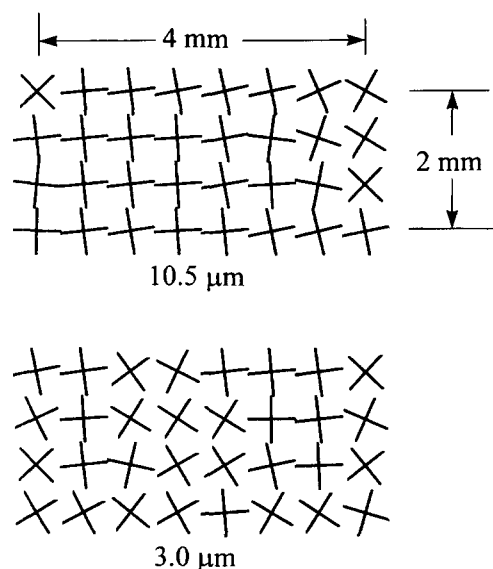


Fig. 5. In-plane alignment of Tl-1223 films. Each cross represents the most common orientation of the $\langle 100 \rangle$ axes in a 0.37 mm^2 area.

- [11] D.J. Miller, J.G. Hu, J.D. Hettinger, K.E. Gray, J.E. Tkaczyk, J. DeLuca, P.L. Karas, J.A. Sutliff and M.F. Garbaskas, *Appl. Phys. Lett.* 63 (1993) 556.
- [12] E.D. Specht, A. Goyal, D.M. Kroeger, J.A. DeLuca, J.E. Tkaczyk, C.L. Briant and J.A. Sutliff, *Physica C* 226 (1994) 76.
- [13] J.E. Tkaczyk, J.A. Sutliff, J.A. DeLuca, P.J. Bednarczyk, C.L. Briant, Z.L. Wang, A. Goyal, D.M. Kroeger, D.H. Lowndes and E.D. Specht, *J. Mater. Res.* 10 (1995) 2203.
- [14] E.D. Specht, A. Goyal, D.M. Kroeger, J.A. DeLuca, J.E. Tkaczyk, C.L. Briant and J.A. Sutliff, *Physica C* 242 (1995) 164.